

Effective charges and virial pressure of concentrated macroion solutions

N. Boon,¹ G. I. Guerrero-García,² R. van Roij,³ and M. Olvera de la Cruz¹

¹*Department of Materials Science and Engineering,
Northwestern University, Evanston, Illinois 60208, USA*

²*Instituto de Física, Universidad Autónoma de San Luis Potosí,
Álvaro Obregón 64, 78000 San Luis Potosí, San Luis Potosí, México*

³*Institute for Theoretical Physics, Center for Extreme Matter and Emergent Phenomena,
Utrecht University, Leuvenlaan 4, 3584 CE Utrecht, The Netherlands*

(Dated: 1 July 2015)

The stability of colloidal suspensions is crucial in a wide variety of processes including the fabrication of photonic materials and scaffolds for biological assemblies. The ionic strength of the electrolyte that suspends charged colloids is widely used to control the physical properties of colloidal suspensions. The extensively used two-body Derjaguin-Landau-Verwey-Overbeek (DLVO) approach allows for a quantitative analysis of the effective electrostatic forces between colloidal particles. DLVO relates the ionic double-layers, which enclose the particles, to their effective electrostatic repulsion. Nevertheless, the double layer is distorted at high macroion volume fractions. Therefore, DLVO cannot describe the many-body effects that arise in concentrated suspensions. We show that this problem can be largely resolved by identifying effective point charges for the macroions using cell theory. This extrapolated point charge (EPC) method assigns effective point charges in a consistent way, taking into account the excluded volume of highly charged macroions at any concentration, and thereby naturally accounting for high volume fractions in both salt-free and added-salt conditions. We provide an analytical expression for the effective pair potential and validate the EPC method by comparing molecular dynamics simulations of macroions and monovalent microions that interact via Coulombic potentials to simulations of macroions interacting via the derived EPC effective potential. The simulations reproduce the macroion-macroion spatial correlation and the virial pressure obtained with the EPC model. Our findings provide a route to relate the physical properties such as pressure in systems of screened-Coulomb particles to experimental measurements.

Coulombic interactions between ionized species affect colloidal suspensions at the microscopic level and have an indirect, yet crucial, impact on the observable macroscopic characteristics of the system[1]. The Derjaguin-Landau-Verwey-Overbeek (DLVO) theory [2, 3], proposed in the 1940's, has been crucial for understanding like-charged colloidal dispersions in a wide variety of experimental conditions. In this theory, the effective pair potential between two equally charged macroions immersed in an electrolyte is expressed as the sum of three terms: a hard-core potential that takes into account the excluded volume of macroions (preventing their overlap), an attractive potential due to short-range (van der Waals) interactions, and an electrostatic screened-Coulomb or Yukawa potential resulting from the linearized Poisson-Boltzmann theory, which is the Debye-Hückel approximation. Many additions and modifications to the original theory have been proposed, including polarization effects, patchiness, or charge regulation, just to mention a few. Special care should be taken for non-aqueous solvents, divalent ions, or high salt concentrations, since in these regimes ion correlations are usually important [4–16]. Generally speaking, modifications to the DLVO theory have been pivotal for systems in which the electrostatics are not well described by the linearized Poisson-Boltzmann theory. Though the DLVO theory has been used extensively to model colloidal dispersions[17], this approach is not exact within the context of the underlying Debye-Hückel approximation. In the precise analysis of the force between two charged spheres in an electrolytic solution, Verwey and Overbeek encountered additional terms that can be considered cross terms, resulting from the exclusion of the ionic double-layer surrounding the first sphere by the hard-core of the second sphere[3]. Numerical methods exist to quantify such effects[18–20], yet these approaches explicitly deal with two particles in an otherwise empty system. While in dilute solutions of macroions the resulting correction to DLVO is typically small and can usually be safely neglected, in dense macroion systems the deviation from DLVO can become very significant due to the overlap between each macroion electrical double-layer with the hard cores of *all* neighbouring particles. As a result, the performance of the classical DLVO equation is limited to the description of dilute systems of macroions [21–25], while many colloidal processes such as crystallization or glass formation predominantly occur in dense systems where many-body effects prevail. Marcelja et al. recognized the importance of many-body effects at high colloidal densities and low electrolyte concentration, and they described a method that uses cell theory to project a charged colloidal dispersion to a system of Coulomb particles[26]. This enabled use of Monte-Carlo simulations of the Wigner lattice to study the crystallization of latex suspensions. That method has recently been rediscovered and extended to charge-regulating particles to describe re-entrant melting on addition of a charging agent to a colloidal suspension[27]. Such an effective Coulomb representation is, however, not

suitable to describe the structure of charged suspensions, particularly in the crystalline phase. This is also true of methods comprising the repulsive forces among macroions via hard sphere interactions with effective hard sphere radii [28–31]. Different approaches such as the (renormalized) Jellium model[32] and methods that calculate the osmotic pressure within a Wigner-Seitz cell[33, 34] have been proposed. However, they do not yield information on the spatial configuration of the macroions and consequently are limited in describing dense macroion systems.

In this work we introduce a method to calculate the effective electrostatic pair interaction between macroions in dense systems through the identification of their corresponding effective point charges. We verify the corresponding accuracy by comparing the resulting radial distribution functions and pressures to the primitive model. To begin, we consider spherical and impenetrable macroions of valence Z and radius a immersed in a 1:1 electrolyte with bulk concentration c_s . Traditionally for dilute macroion systems, the non-linear Poisson-Boltzmann (PB) theory establishes that the electrostatic potential is described by $\nabla^2\Phi(\mathbf{r}) = \kappa_{\text{res}}^2 \sinh\Phi(\mathbf{r})$ outside the macroion, where $\Phi(\mathbf{r}) = \Psi(\mathbf{r})e/k_B T$, $\Psi(\mathbf{r})$ is the electrostatic potential, e is the elementary charge, and $k_B T$ is the thermal energy of the solution. The parameter $\kappa_{\text{res}} = \sqrt{8\pi\lambda_B c_s}$ is an inverse screening length depending on the Bjerrum length $\lambda_B \equiv e^2/(k_B T \epsilon)$, where ϵ is the relative dielectric permittivity. For sufficiently small charges, the PB equation can be linearized by using $\sinh\Phi(\mathbf{r}) \approx \Phi(\mathbf{r})$, resulting in the Debye-Hückel approximation, $\nabla^2\Phi(\mathbf{r}) = \kappa_{\text{res}}^2 \Phi(\mathbf{r})$. The electrostatic potential outside the macroion is found to be $\Phi(r) = \lambda_B Q_{\text{DLVO}} \exp(-\kappa_{\text{res}} r)/r$, with $r > a$ the distance to the center of the particle and $Q_{\text{DLVO}} \equiv Z \exp(\kappa_{\text{res}} a)/(1 + \kappa_{\text{res}} a)$. The electric field, and thus the electrostatic force it exerts on a test charge[35], is the same as that of a point particle with charge Q_{DLVO} . One can therefore identify Q_{DLVO} as the effective point charge in the DLVO theory and estimate the pair potential between two macroions from the screened Coulomb interaction of two point charges at a distance D ,

$$\frac{U(D)}{k_B T} = Q^2 \lambda_B \frac{\exp(-\kappa D)}{D}, \quad (1)$$

with $Q = Q_{\text{DLVO}}$ and $\kappa = \kappa_{\text{res}}$ according to DLVO theory.

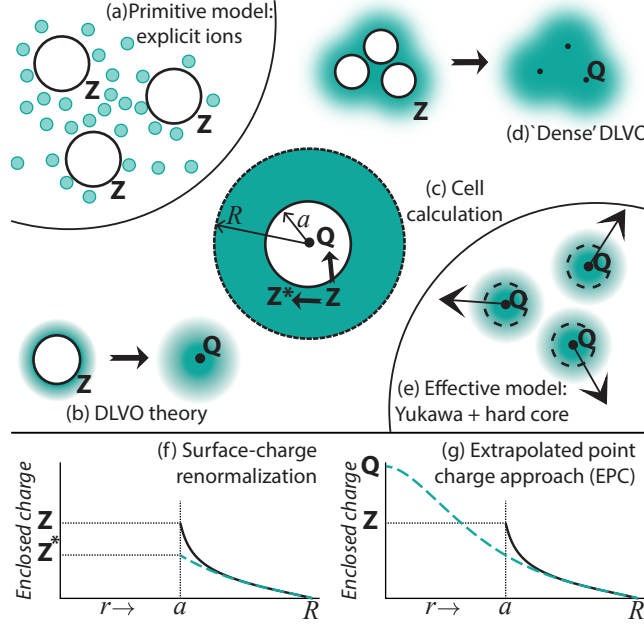


FIG. 1: The various paths (b,c,d) from the primitive model (a) of monovalent microions and macroions of valency Z to the effective model (e) where interactions are hard-core Yukawa with effective point charges Q . (f) and (g) show PB-cell calculations for the electric field (or charge within radius r) around a macroion following from nonlinear calculations (full line) and the Debye-Hückel fit (dashed line); (f) illustrates how surface charge renormalization yields a charge Z^* that can be inserted into DLVO theory. In the extrapolated point charge approach, the effective point charge Q is calculated directly from the extrapolation displayed in (g).

Apart from being restricted to dilute systems, the DLVO equation above cannot directly be applied to strongly charged macroions, since the Debye-Hückel approximation no longer holds for these systems, which strictly speaking leads to non-pairwise additive interaction potentials [36, 37]. Alexander and collaborators[33], however, showed

that nonlinear ion behavior close to the macroion surface can be embodied in an effective linear-screening model by calculating a renormalized surface charge Z^* that, far away from the charged macroion surface, induces the same electrostatic potential and electric field as would be obtained within the non-linear PB equation [33, 38–42], see Fig. 1f. Regarding a system of macroions at a concentration ρ_M and macroion packing fraction $\eta = 4\pi\rho_M a^3/3$, each of the macroions is imagined to be in the center of a charge-neutral spherical cell with radius $R = a\eta^{-1/3}$, such that the summed volume of all cells match the system's volume[21]. This is illustrated in Fig. 1c. In this spherical geometry, the non-linear PB equation and the associated boundary conditions can be written as

$$\Phi''(r) + \frac{2\Phi'(r)}{r} = \kappa_{\text{res}}^2 \sinh \Phi(r); \quad (2a)$$

$$\Phi'(a) = -\frac{Z\lambda_B}{a^2}; \quad \Phi'(R) = 0, \quad (2b)$$

where the prime denotes a derivative with respect to r . The boundary conditions follow from Gauss' law and include the global electroneutrality condition of the whole system. This set of equations is typically solved numerically as no general analytical solution is known. Once the numerical solution is determined, one proceeds by linearizing Eq. (2a) around the obtained potential at the cell boundary, which can be regarded as the Donnan potential, $\Phi_D \equiv \Phi(R)$. This yields the Debye-Hückel approximation $\Phi_\ell''(r) + 2\Phi_\ell'(r)/r = \kappa^2 \Phi_\ell(r)$ for the shifted potential $\Phi_\ell(r) \equiv (\Phi(r) - \Delta\Phi)$, with $\Delta\Phi = \Phi_D - \tanh \Phi_D$, and the screening parameter $\kappa = \kappa_{\text{res}} \sqrt{\cosh \Phi_D}$. Analytical solutions to the linearized PB equation are $\Phi_\ell(r) \equiv a_+ e^{+\kappa r}/r + a_- e^{-\kappa r}/r$. These form an accurate approximation to the nonlinear profile in the proximity of the cell's boundary if one chooses $a_\pm = \exp(\mp \kappa R) \tanh \Phi_D$ ($\kappa R \pm 1$)/(2 κ), where the latter follows from the constraints $\Phi_\ell(R) + \Delta\Phi = \Phi_D$ and $\Phi_\ell'(R) = 0$. The effective surface charge can now be extracted from the derivative of the analytical approximation at $r = a$, i.e., $Z^* \equiv -\Phi_\ell'(a)a^2/\lambda_B$ (see Fig. 1(f)), and one finds $Z^* = a_+/\lambda_B(\kappa a - 1)e^{+\kappa a} - a_-/\lambda_B(\kappa a + 1)e^{-\kappa a}$ [43]. Then, using κ and Z^* as parameters, the effective interactions between the macroions can be estimated by using the DLVO theory again.

The accuracy and simplicity of the previous cell-model approach can, however, be improved by calculating an effective *point* charge Q *directly* through identification of a point charge at $r = 0$ by extrapolating the analytical approximation (see Fig. 1(g)), yielding the form $Q \equiv \lim_{r \rightarrow 0} -\Phi_\ell'(r)r^2/\lambda_B = (a_+ + a_-)/\lambda_B$. The latter can also be expressed as

$$Q = \frac{\tanh \Phi_D}{\kappa \lambda_B} [\kappa R \cosh \kappa R - \sinh \kappa R]. \quad (3)$$

The parameters κ and Q can then be used to approximate the effective electrostatic interactions in the original macroion system by those of point charges, using Eq. (1) to find the pairwise interaction energy. Although high macroion volume fractions render DLVO-based approaches inaccurate[21–25], the effective system of point charges has no hard-core volumes that will overlap with ionic double layers. We therefore expect that Eq. (3) in combination with Eq. (1) will remain accurate even in dense macroion systems. Note that the hard-core repulsions for $D < 2a$ should be maintained for the non-electrostatic part of the pair interactions. Hereafter, we refer to the latter approach as the extrapolated point charge (EPC) method. The theoretical motivation for this approach is that screened-Coulomb or Yukawa potentials solve the screened Poisson equation *without* considering the hard-core contribution of macroions at finite concentration. Thus the main advantage of the EPC method is that it defines effective point charges in a consistent way, taking into account the excluded volume of highly charged macroions at any concentration.

In the regime where Z is small and the resulting potential profile is sufficiently flat throughout the cell, $|\Phi(R) - \Phi(a)| \ll 1$, the analytical approximations to Eq. (3) will become exact on the entire space between the cell boundary and the macroion surface. As a consequence a_\pm can be calculated from $\Phi_\ell'(a) = -Z\lambda_B/a^2$ and $\Phi_\ell'(R) = 0$ and a direct analytical relation between Z and Q follows (Fig. 1d). Tantalizingly, inserting this Q into Eq. (1) yields a pair potential similar to the DLVO equation,

$$\frac{U(D)}{k_B T} = \frac{Z^2 \lambda_B e^{-\kappa D} [2e^{-\kappa(R-a)} (\kappa R \cosh \kappa R - \sinh \kappa R)]^2}{D [(1+\kappa a)(\kappa R-1) + (1-\kappa a)(\kappa R+1)e^{-2\kappa(R-a)}]^2}, \quad (4)$$

for $D \geq 2a$, and $V(D) = \infty$ for $D < 2a$. The screening parameter κ that enters Eq. (4) reduces to the reservoir value κ_{res} for systems with a sufficient amount of added salt, for which $|\Phi_D| \ll 1$. Recall that $R = a\eta^{-1/3}$ and that classical (η -independent) DLVO theory is re-obtained for dilute suspensions, which is the limit $R \rightarrow \infty$. For completeness we confirm that in the limit of large double-layer size, $\kappa^{-1} \gg D$, Eq. (4) reduces to the Coulombic form $U(D)/k_B T = (Z/(1-\eta))^2 \lambda_B/D$, with an effective charge $Z/(1-\eta)$ that is larger than the bare charge Z due to the

expulsion of the ionic background from the hard core[26, 27, 44–46].

To verify our proposed prescription, molecular dynamic (MD) simulations of macroion/microion mixtures with particle diameters $d_M = 2a = 750$ Å, and $d_+ = d_- = 3$ Å, respectively, were performed in the constant number, volume, and temperature (NVT) ensemble using the Large-scale Atomic/Molecular Massively Parallel Simulator (LAMMPS) package [47]. This extreme size-asymmetry between macroions and microions is selected to mimic realistic experimental colloidal systems. Macroions and monovalent microions, fulfilling the electroneutral condition, were placed inside a cubic simulation box of length L under periodic boundary conditions. In the primitive-model (PM) representation that we applied here, ionic species are represented by repulsive-core spheres with point charges in their centers immersed in a continuous solvent [48–51]. The pairwise forces among all particles have a short-range repulsive-core potential component, $u_{ij}^{rc}(D)$, and a long-ranged Coulombic pair potential contribution, $u_{ij}^{el}(D)/k_B T = \lambda_B z_i z_j / D$, where z_i and z_j are the valences associated to particles i and j , respectively. These interactions are handled properly, using the particle-mesh Ewald technique[52]. We model the repulsive-core pair potential between a particle of species i and a particle of species j , separated by a distance D , as an impenetrable hard-core $u_{ij}^{rc}(D) = \infty$ for $D \leq \Delta_{ij}$, a shifted-truncated Lennard-Jones potential $u_{ij}^{rc}(D)/k_B T = 4 [(\sigma/(D - \Delta_{ij}))^{12} - (\sigma/(D - \Delta_{ij}))^6] + 1$ for $\Delta_{ij} < D < \Delta_{ij} + 2^{1/6}\sigma$, and by a potential $u_{ij}^{rc}(D) = 0$ for $D \geq \Delta_{ij} + 2^{1/6}\sigma$, where $\Delta_{ij} = (d_i + d_j)/2 - \sigma$ is the hard-core diameter. The parameter σ regulates the hardness of the repulsive-core interactions. To mimic the hard core interaction characteristic of the primitive model, σ is set equal to 0.1 nm. We use $\lambda_B = 7.143$ Å throughout the text for theoretical and simulation calculations. Additional details of the simulation setup can be found in Refs. [49–51].

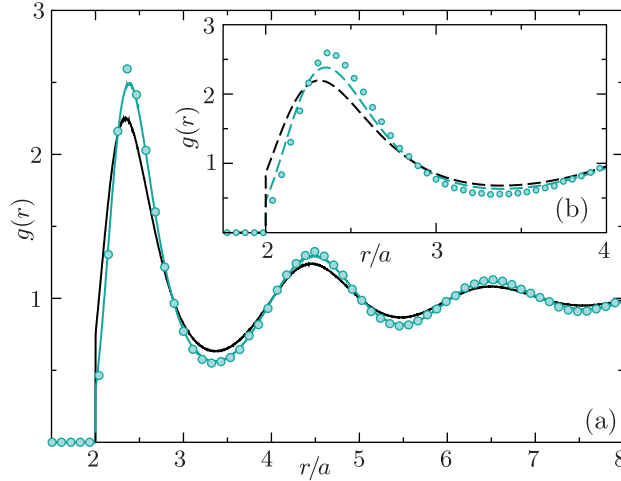


FIG. 2: Comparison of the pair correlation between macroions resulting from the full-ion primitive-model MD simulations (circles) with those obtained by using repulsive-core effective screened-Coulomb models (lines), relying on the the EPC approach (green) and surface charge renormalization approach (black). The solid lines (a) represent MD simulations results whereas the dashed lines in the inset (b) were obtained from the Ornstein-Zernike equation within the Rogers-Young closure; both (a) and (b) correspond to the same system in which the valence and packing fraction of the macroions in the primitive model are $Z = 80$, and $\eta = 0.3682$, respectively.

In Fig. 2 we compare radial distributions from computationally expensive primitive-model MD simulations (circles) to much faster and economic effective-model descriptions using MD simulations (main figure, solid lines), and integral equations (inset, dashed lines). In the primitive-model approach we use a cubic simulation box of length $L = 8d_M = 6000$ Å, containing 360 macroions of valence $Z = 80$, 31680 small monovalent counterions ($-e$), and 2880 small monovalent co-ions ($+e$). In the effective-model approach, microions are included implicitly in the Yukawa interactions between macroions with an effective charge Q and inverse screening length κ . The charges associated to the macroion profiles shown in Fig. 2 are $Q = 204$ following the EPC approach and $Q = 167$ following the surface charge renormalization approach in combination with the DLVO theory. An excellent agreement between the heavy-duty primitive-model results, in which microions are included explicitly, and the computationally inexpensive MD Yukawa simulations using the EPC prescription can be observed in Fig. 2(a). In contrast, surface charge renormalization in combination with the DLVO theory deviates significantly from primitive-model simulation results, as expected at this volume fraction. The use of integral equations theory allows for an even faster numerical

calculation of the radial distribution functions within the effective model. The Rogers-Young(RY) closure[53], which is known for its superb accuracy for hard-core Yukawa systems[46, 54–56], has good qualitative agreement compared with primitive-model results, as can be seen in Fig. 2 (b). Note that PB techniques are grand canonical and therefore require a reservoir ion density c_s or screening parameter κ_{res} , while the number of ions in the primitive-model system is fixed, as there is no particle exchange with a reservoir. Therefore, we add an additional step to our PB method to obtain canonical results: for any choice of c_s we integrate the resulting ion profiles in the cell, which yields the total number of ions per macroion. The latter can be compared with the number of ions per macroion in the simulation box. Subsequently, the right value for c_s is determined by a root-finding procedure with respect to their difference.

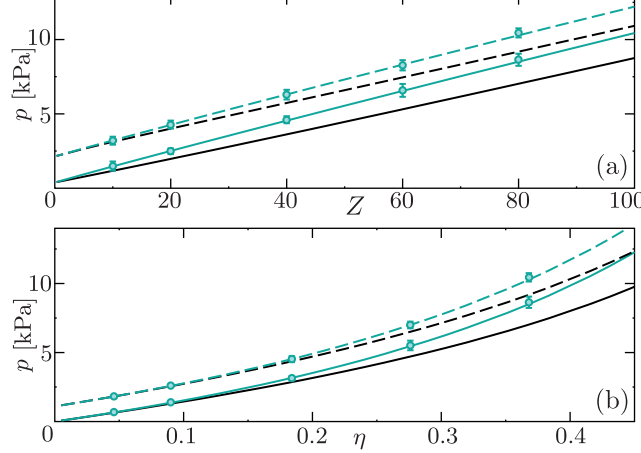


FIG. 3: The total pressure in the macroion/microion mixture as a function of (a) Z for a fixed macroion volume fraction $\eta = 0.3682$, and as a function of (b) η and for $Z = 80$. Both graphs show data for both the salt-free (solid, lower set of lines and circles) and the added-salt case (dashed, upper set of lines and circles), in which 2880 extra cations and 2880 extra anions were added. The lines result from RY-calculations using the effective model parameters following from the EPC approach (green) or surface charge renormalization approach (black). The circles show the results of primitive-model simulations and error bars are included for those cases where the error is larger than the circle size.

The total microion/macroion pressure resulting from the primitive model, p_{PM} , as well as the macroion pressure in the effective model, p_{EM} , can be calculated via the virial equation $p = \frac{N}{V}k_B T + \frac{1}{3V} \langle \sum_{i < j}^N D_{ij} \cdot U'_{ij}(D_{ij}) \rangle$, where N sums all particles, in the primitive model, or only the macroions, in the effective model, and $U'_{ij}(D_{ij})$ is the derivative with respect to the distance D_{ij} of the (un)screened Coulomb pair interaction between particles i and j . However, to relate p_{EM} to p_{PM} it is essential to include a correction term which can be regarded as the pressure of a homogeneous background of counterions and co-ions,

$$p_{\text{PM}} \approx p_{\text{EM}} + k_B T \frac{\kappa^2}{8\pi\lambda_B} \left(1 + \frac{\kappa_{\text{res}}^4}{\kappa^4} \right). \quad (5)$$

Density functional theory[21, 22, 25, 57] may be applied for a rigorous derivation of this pressure difference, which shows up as a volume term in the free energy of the effective system[22, 58–60]. We refer to the supplementary material for this. Note that Eq. (5) implies that the macroion osmotic pressure, which is the pressure with respect to the ion reservoir, $\Pi = p_{\text{PM}} - 2c_s k_B T$ [34], does not equal p_{EM} in general; only if κ approaches κ_{res} , the pressure difference in Eq. (5) reduces to $k_B T \kappa_{\text{res}}^2 / (4\pi\lambda_B) = 2c_s k_B T$.

Fig. 3 shows the primitive-model pressure p_{PM} resulting from primitive-model simulations, as well as the effective-model approximations following from Eq. (5) applying the RY closure. Even though the agreement between the radial distribution functions obtained from the EPC method using the RY closure and the primitive model simulations is not as accurate as that obtained from the EPC effective screened Coulomb simulations (see e.g., Fig. 2), we have observed that the virial pressure obtained from the RY closure and the effective screened Coulomb simulations using the EPC approach agreed with the pressure p_{PM} obtained from the primitive-model simulations within the corresponding numerical uncertainty. One observes superior accuracy of EPC with respect to the surface charge renormalization approach for a wide range in Z (a), and in particular for high η (b). While the dashed lines in Fig. 3 represent added salt cases, the full lines correspond to a system without co-ions, i.e. a salt-free ‘reservoir’: $c_s = \kappa_{\text{res}}^2 / (8\pi\lambda_B) = 0$

[61, 62], for which Eqs. (2a) and (2b) in principle cannot be solved. Our cell calculations, however, show that the salt-free limit $\kappa_{\text{res}} \rightarrow 0$ is perfectly well defined and can be characterized by the condition that the number of co-ions is negligible with respect to the counterions. For small κ_{res} , all relevant physical quantities such as the number of ions per macroion, Q , and κ converge to their values in a salt-free environment. Salt-free cases therefore do not require a root-finding procedure w.r.t κ_{res} , but instead can be considered by choosing κ_{res} sufficiently small such that $\kappa_{\text{res}}/\kappa \ll 1$, i.e. $\Phi_D \gg 1$. For small macroion charges, $Z\lambda_B/a < 1$, we find that the resulting physical κ is in accordance with a homogeneous distribution of neutralizing counterions, $\kappa^2 = 3Z\lambda_B\eta/(a^3(1-\eta))$ [21, 44, 45, 62]. This, in combination with Eq. (4), yields a description at any density of the pair interactions in salt-free systems depending on Z , λ_B , a and η only. The pressure correction in Eq. (5) reduces to $k_B T \kappa^2 / 8\pi\lambda_B$. The strong dependence of κ on η , is particularly important in other geometries, such as the charged two-plate system, from what we study here. In the latter, the distance between the plates also sets the system's volume and therefore κ , yielding a non-exponential form for the pair-potential [63]. However, for macroion suspensions this is not the case, as η is a fixed parameter independent of the configuration.

In this work we have introduced a method that extends the capabilities of the DLVO theory to high valences and volume fractions of colloidal macroions using no additional assumptions besides the underlying Poisson-Boltzmann theory. Akin to the original theory, this approach is mainly applicable to systems with monovalent microions for which ion correlations are unimportant, although approximate extensions to systems with correlated multivalent counterions might be obtainable. We also propose a route to relate the pressure in the effective system of macroions to the osmotic pressure that can be measured experimentally in colloidal systems, for example in sedimentation profiles [64, 65]. Our method demonstrates accuracy with respect to acquiring the measurable properties of charged colloidal suspensions, and can therefore be applied to guide and interpret experiments on related systems.

ACKNOWLEDGEMENTS

We thank the support of the Center for Bio-Inspired Energy Science (CBES), which is an Energy Frontier Research Center funded by the U.S. Department of Energy, Office of Science, Basic Energy Sciences under Award DESC0000989. G.I.G.-G. acknowledges the Mexican National Council of Science and Technology (CONACYT) for the financial support via the program ‘‘Catedras CONACYT’’. The computer cluster where part of the simulations were performed was funded by the Office of the Director of Defense Research and Engineering (DDR&E) and the Air Force Office of Scientific Research (AFOSR) under Award no. FA9550-10-1-0167. This work is part of the D-ITP consortium, a program of The Netherlands Organisation for Scientific Research (NWO), that is funded by the Dutch Ministry of Education, Culture and Science (OCW).

-
- [1] I. Langmuir, The Journal of Chemical Physics **6**, 873 (1938).
 - [2] B. Derjaguin and L. Landau, Acta Physicochim. URSS **14**, 633 (1941).
 - [3] E. J. W. Verwey and J. T. G. Overbeek, *Theory of the Stability of Lyophobic Colloids* (Elsevier, New York, 1948).
 - [4] S. Levine, J. Mingins, and G. Bell, Journal of Electroanalytical Chemistry and Interfacial Electrochemistry **13**, 280 (1967).
 - [5] F. H. Stillinger Jr and J. G. Kirkwood, The Journal of Chemical Physics **33**, 1282 (1960).
 - [6] S. Levine, C. W. Outhwaite, and L. B. Bhuiyan, Journal of Electroanalytical Chemistry and Interfacial Electrochemistry **123**, 105 (1981).
 - [7] L. Blum, The Journal of Physical Chemistry **81**, 136 (1977).
 - [8] J. Valleau, R. Ivkov, and G. Torrie, The Journal of chemical physics **95**, 520 (1991).
 - [9] F. Oosawa, Polyelectrolytes, in *Polyelectrolytes*, Marcel Dekker, 1971.
 - [10] D. Henderson, Fluid phase equilibria **76**, 1 (1992).
 - [11] X. Chu and D. T. Wasan, Journal of colloid and interface science **184**, 268 (1996).
 - [12] R. R. Netz and H. Orland, The European Physical Journal E **1**, 203 (2000).
 - [13] A. Z. Panagiotopoulos and M. E. Fisher, Physical review letters **88**, 045701 (2002).
 - [14] R. Kjellander, Berichte der Bunsengesellschaft für physikalische Chemie **100**, 894 (2010).
 - [15] E. Wernersson, R. Kjellander, and J. Lyklema, The Journal of Physical Chemistry C **114**, 1849 (2010).
 - [16] J. W. Zwanikken and M. O. de la Cruz, Proceedings of the National Academy of Sciences **110**, 5301 (2013).
 - [17] B. Ninham, Adv. Colloid and Interface Sci. **83**, 1 (1999).
 - [18] A. Glendinning and W. Russel, Journal of colloid and interface science **93**, 95 (1983).
 - [19] S. L. Carnie, D. Y. Chan, and J. Stankovich, Journal of colloid and interface science **165**, 116 (1994).
 - [20] P. Warszyński and Z. Adamczyk, Journal of colloid and interface science **187**, 283 (1997).
 - [21] H. H. von Grünberg, R. van Roij, and G. Klein, Europhys. Lett. **55**, 580 (2001).

- [22] R. van Roij and J. P. Hansen, Phys. Rev. Lett. **79**, 3082 (1997).
- [23] P. B. Warren, J. Chem **112**, 4683 (2000).
- [24] H. Löwen, P. A. Madden, and J. P. Hansen, Phys. Rev. Lett. **68**, 1081 (1992).
- [25] J. P. Hansen and H. Löwen, Annu. Rev. Phys. Chem. **51**, 209 (2000).
- [26] S. Marcelja, D. Mitchell, and B. Ninham, Chemical Physics Letters **43**, 353 (1976).
- [27] T. Kanai *et al.*, Phys. Rev. E (2015).
- [28] D. Stigter, Recueil des Travaux Chimiques des Pays-Bas **73**, 593 (1954).
- [29] W. van Megen and I. Snook, Chemical Physics Letters **35**, 399 (1975).
- [30] S. L. Brenner, The Journal of Physical Chemistry **80**, 1473 (1976).
- [31] J. A. Beunen and L. R. White, Colloids and Surfaces **3**, 371 (1981).
- [32] E. Trizac and Y. Levin, Phys. Rev. E **69**, 031403 (2004).
- [33] S. Alexander *et al.*, J. Chem. Phys. **80**, 5776 (1984).
- [34] V. Reus, L. Belloni, T. Temb, N. Lutterbach, and D. Versmold, J. Phys. II France **7**, 603 (1997).
- [35] D. Griffiths, *Introduction to electrodynamics* (Prentice Hall Upper Saddle River, NJ, 1999).
- [36] J. Dobnikar, Y. Chen, R. Rzehak, and H. H. von Grünberg, J. Chem. Phys. **119**, 4971 (2003).
- [37] J. Dobnikar, R. Castañeda Priego, H. H. von Grünberg, and E. Trizac, New. J. Phys. **8**, 277 (2006).
- [38] L. Belloni, Colloids Surf., A **140**, 227 (1997).
- [39] E. Trizac, L. Bocquet, and M. Aubouy, Phys. Rev. Lett. **89**, 248301 (2002).
- [40] E. Trizac, L. Bocquet, M. Aubouy, and H. H. von Grünberg, Langmuir **19**, 4027 (2003).
- [41] A. Diehl and Y. Levin, J. Chem. Phys. **121**, 12100 (2004).
- [42] A. R. Denton, J. Phys. Condens. Matter **22**, 364108 (2010).
- [43] B. Zoetkouw, *Phase behavior of charged colloids*, PhD thesis, Utrecht University, 2006.
- [44] W. B. Russel and D. W. Benzing, J. Colloid Interface Sci. **83**, 163 (1981).
- [45] A. R. Denton, Phys. Rev. E **62**, 3855 (2000).
- [46] M. Heinen, P. Holmqvist, A. J. Banchio, and G. Nägele, J. Chem. Phys. **134**, 129901 (2011).
- [47] S. Plimpton, J. Comput. Phys. **117**, 1 (1995).
- [48] A.-P. Hynninen and M. Dijkstra, J. Chem. Phys. **123**, 244902 (2005).
- [49] P. González-Mozuelos, G. I. Guerrero-García, and M. Olvera de la Cruz, J. Chem. Phys. **139**, 064709 (2013).
- [50] G. I. Guerrero-García, P. González-Mozuelos, and M. Olvera de la Cruz, ACS nano **7** (**11**), 9714 (2013).
- [51] G. I. Guerrero-García and M. Olvera de la Cruz, J. Phys. Chem. B **118**, 8854 (2014).
- [52] T. Darden, D. York, and L. Pedersen, J. Chem. Phys. **98**, 10089 (1993).
- [53] F. J. Rogers and D. A. Young, Phys. Rev. A **30**, 999 (1984).
- [54] R. Castañeda Priego, L. F. Rojas-Ochoa, V. Lobaskin, and J. C. Mixteco-Sánchez, Phys. Rev. E **74**, 051408 (2006).
- [55] J. Gapinski, G. Nägele, and A. Patkowski, J. Chem. Phys. **136**, 024507 (2012).
- [56] S. Zhou and X. Zhang, J. Phys. Chem. B **107**, 5294 (2003).
- [57] R. Evans, Adv. Phys. **28**, 143 (1979).
- [58] H. Graf and H. Löwen, Phys. Rev. E **57**, 5744 (1998).
- [59] B. Zoetkouw and R. van Roij, Phys. Rev. E **73**, 021403 (2006).
- [60] B. Zoetkouw and R. van Roij, Phys. Rev. Lett. **97**, 258302 (2006).
- [61] S. Sainis, J. W. Merrill, and E. R. Dufresne, Langmuir **24**, 13334 (2008).
- [62] H. Ohshima, J. Colloid Interface Sci. **247**, 18 (2002).
- [63] W. H. Briscoe and P. Attard, J. Chem. Phys. **117**, 5452 (2002).
- [64] A. Torres, A. Cuetos, M. Dijkstra, and R. van Roij, Phys. Rev. E **77**, 031402 (2008).
- [65] C. P. Royal, R. van Roij, and A. van Blaaderen, J. Phys. Condens. Matter **17**, 2315 (2005).

SUPPLEMENTARY MATERIAL

Here we will demonstrate how the pressure difference between the effective Yukawa model and the primitive model, as stated in Eq.(5) of the main text, can be derived. We consider a very general charge distribution $q(\mathbf{r})$ without hard core volume, which is in osmotic contact with a reservoir of point ions, the latter having a total density of $2c_s$. Within local mean-field approximation, the effective Hamiltonian of such a system can be calculated from the ion profiles $\rho_{\pm}(\mathbf{r})$ as [21]

$$\frac{\Omega}{k_B T} = \sum_{\alpha=\pm} \int d\mathbf{r} \rho_{\alpha}(\mathbf{r}) \left[\log \frac{\rho_{\alpha}(\mathbf{r})}{c_s} - 1 \right] + \frac{1}{2} \int d\mathbf{r} [\rho_+(\mathbf{r}) - \rho_-(\mathbf{r}) + q(\mathbf{r})] \Phi(\mathbf{r}). \quad (6)$$

Here, the first term in the integrand can be regarded as the contribution from the ionic entropy and the second term the electrostatic energy density of the charge configuration. Note that $\log c_s = \beta \mu_{\pm} \Gamma_{\pm}^{-3}$, with μ_{\pm} the ionic chemical potential and Γ_{\pm} their thermal wavelength. The electrostatic potential is defined as $\Phi(\mathbf{r}) = \lambda_B \int d\mathbf{r}' [\rho_+(\mathbf{r}') - \rho_-(\mathbf{r}') + q(\mathbf{r}')] / \epsilon_0$. Minimization of Eq. (6) w.r.t. the ion densities $\rho_{\pm}(\mathbf{r})$ yields the PB equation, $\nabla \Phi(\mathbf{r}) = \kappa_{\text{res}}^2 \sinh \Phi(\mathbf{r}) - 4\pi q(\mathbf{r})$. In general the latter nonlinear equation cannot be solved analytically; however if we assume the ion densities to be sufficiently close to a yet undetermined density $\tilde{\rho}$, then the integrand in Eq. (6) can be approximated as a quadratic function of $(\rho_{\pm}(\mathbf{r}) - \tilde{\rho}_{\pm})$. We obtain

$$\frac{\Omega_{\ell}}{k_B T} = -\frac{V}{2} (\tilde{\rho}_+ + \tilde{\rho}_-) + \sum_{\alpha=\pm} \int d\mathbf{r} \rho_{\alpha}(\mathbf{r}) \left(\log \frac{\tilde{\rho}_{\alpha}}{c_s} - 1 \right) + \frac{1}{2\tilde{\rho}_{\alpha}} \rho_{\alpha}(\mathbf{r})^2 + \int d\mathbf{r} \frac{1}{2} [\rho_+(\mathbf{r}) - \rho_-(\mathbf{r}) + q(\mathbf{r})] \Phi(\mathbf{r}), \quad (7)$$

with V the system's volume. For a specific macroion/microion mixture, we determine $\tilde{\rho}_{\pm}$ and $q(\mathbf{r})$ following the cell approach that was described in the main text. The effective point charge Q yields a charge distribution $q(\mathbf{r}) = \sum_{i \leq M} Q \delta^3(\mathbf{r}_i - \mathbf{r})$ for M macroions, and we choose $\tilde{\rho}$ to be the ion densities at the cell surface, $\tilde{\rho}_{\pm} \equiv \rho(R) = c_s \exp(\mp \Phi_D)$. As a result Eq. (7) may be transformed into

$$\begin{aligned} \frac{\Omega_{\ell}}{k_B T} = & -V \frac{c_s}{\cosh \Phi_D} (1 + \cosh^2 \Phi_D) + \sum_{\alpha=\pm} \int d\mathbf{r} \frac{\exp(\alpha \Phi_D)}{2c_s} (\rho_{\alpha}(\mathbf{r}) - \tilde{c}_s)^2 \\ & + \int d\mathbf{r} \frac{1}{2} [\rho_+(\mathbf{r}) - \rho_-(\mathbf{r}) + q(\mathbf{r})] (\Phi_{\ell}(\mathbf{r}) - \Delta \Phi) + \int d\mathbf{r} q(\mathbf{r}) \Delta \Phi, \end{aligned} \quad (8)$$

where $\Delta \Phi = \Phi_D - \tanh \Phi_D$, $\tilde{c}_s = c_s / \cosh \Phi_D$, and $\Phi_{\ell}(\mathbf{r}) = \Phi(\mathbf{r}) - \Delta \Phi$ is the shifted electrostatic potential. From the functional derivatives $\frac{\delta \Omega_{\ell}}{\delta \rho_{\pm}} = 0$ we find $\rho_{\pm}(\mathbf{r}) = \tilde{c}_s \mp c_s \exp(\mp \Phi_D) \Phi_{\ell}(\mathbf{r})$ and now the Debye-Hückel approximation for the shifted potential $\Phi_{\ell}(\mathbf{r})$ is recovered, $\nabla \Phi_{\ell}(\mathbf{r}) = \kappa^2 \Phi_{\ell}(\mathbf{r}) - 4\pi \lambda_B q(\mathbf{r})$, with the effective screening parameter $\kappa^2 = \kappa_{\text{res}}^2 \cosh \Phi_D$. Our choice is self-consistent since the latter equation reduces to a cell model in which $\Phi_{\ell}''(r) + \Phi_{\ell}'(r)/2r = \kappa^2 \Phi_{\ell}'(r)$, with $\Phi_{\ell}'(R) = 0$ and $\lim_{r \rightarrow 0} \Phi_{\ell}'(r)r^2 = -Q\lambda_B$, describes the cell potential profiles. This reproduces the analytical approximation to the ion profiles within the cell, and therefore validates our choice of $\tilde{\rho}_{\pm}$ a posteriori. For the general distribution of effective point charges, one finds the electrostatic potential $\Phi_{\ell}(\mathbf{r}) = \sum_{i \leq M} Q \lambda_B \exp(-\kappa |\mathbf{r} - \mathbf{r}_i|) / |\mathbf{r} - \mathbf{r}_i|$, and therefore

$$\frac{U_{\text{EL}}}{k_B T} = \sum_{i < j} \frac{Q^2 \lambda_B}{|\mathbf{r}_i - \mathbf{r}_j|} \exp(-\kappa |\mathbf{r}_i - \mathbf{r}_j|) + M(Q \Delta \Phi) - V \frac{\kappa^2}{8\pi \lambda_B} \left(\frac{\kappa_{\text{res}}^4}{\kappa^4} + 1 \right), \quad (9)$$

gives the electrostatic energy of the effective macroion system. Note that divergent self-energy terms are omitted. Now, the electrostatic pressure can be obtained by the usual derivative w.r.t. V , choosing to keep $\tilde{\rho}_{\pm}$ constant since those remain appropriate fixed points in the quadratic approximation to Eq. (6) for infinitesimal changes of V . We obtain

$$p = \left(\frac{dU_{\text{EL}}}{dV} \right)_{M, T, \tilde{\rho}_{\pm}} = p_Y + k_B T \frac{\kappa^2}{8\pi \lambda_B} \left(\frac{\kappa_{\text{res}}^4}{\kappa^4} + 1 \right). \quad (10)$$

Here, p_Y is the usual electrostatic pressure of the set of point charges that interact via an Yukawa interaction, whilst the second term reveals an additional contribution to the electrostatic pressure. Therefore, this is the additional pressure that must be added to the total pressure of the effective (hard-core) Yukawa system to relate to the primitive-model pressure which includes both macroions and microions explicitly.